

CrossMark
click for updatesCite this: *Phys. Chem. Chem. Phys.*,
2016, **18**, 5883Received 14th December 2015,
Accepted 25th January 2016

DOI: 10.1039/c5cp07709e

www.rsc.org/pccp

Progress in the theory of electrostatic interactions between charged particles

Eric B. Lindgren, Ho-Kei Chan,† Anthony J. Stace* and Elena Besley*

In this perspective we examine recent theoretical developments in methods for calculating the electrostatic properties of charged particles of dielectric materials. Particular attention is paid to the phenomenon of like-charge attraction and we investigate the specific conditions under which particles carrying the same sign of charge can experience an attractive interaction. Given favourable circumstances, it is shown that even weakly polarisable materials, such as oil droplets and polymer particles, can experience like-charge attraction. Emphasis is also placed on the numerical accuracy of the multipole approach adopted in many electrostatic solutions and on the importance of establishing strict convergence criteria when addressing problems involving particulate materials with high dielectric constants.

Introduction

Electrostatic interactions between charge particles impact on many natural phenomena and human activities. Examples of the former include cloud formation and the behaviour of volcanic ash,^{1–3} whilst in the latter category, powder coating,⁴ printing,⁵ food processing,⁶ and charge scavenging in coal-fired power stations,⁷

can be included in a long list of applications where particles are deliberately charged in order to facilitate particular industrial processes or operations.⁸ Underpinning all of these examples is the need to developing a quantitative understanding of the electrostatic interactions that exist between charged particles of widely varying composition. Early research on this topic, focused primarily on conducting spheres, derives from the work of W. Thomson (also known as Lord Kelvin) and was aided by comparatively simple boundary conditions and driven by a desire to better understand the emerging field of electrostatics.⁹ A complete solution to the interaction between two conducting spheres did not appear until 1964 when Davis used a bispherical coordinate system to derive an expression for the

Department of Theoretical and Physical Chemistry, School of Chemistry, University of Nottingham, University Park, Nottingham, NG7 2RD, UK.

E-mail: tony.stace@nottingham.ac.uk, elena.besley@nottingham.ac.uk

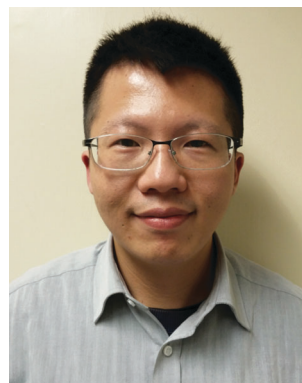
† Current address: Shenzhen Graduate School, The Harbin Institute of Technology, Shenzhen, China.



Eric B. Lindgren

Eric Brazil Lindgren was awarded his MSci degree in Chemistry in 2013 from the Fluminense Federal University, Brazil. In the same year he was awarded a “Science without Borders” scholarship from the Brazilian Government and started his PhD under the supervision of Prof. Elena Besley in the computational materials and nano-science group at the University of Nottingham. His current research focuses on the study of

electrostatic interactions between charged particles using state-of-the-art modeling approaches.



Ho-Kei Chan

Ho-Kei Chan has recently joined the Shenzhen Graduate School of the Harbin Institute of Technology as an Associate Professor. He obtained a first class BSc degree in Engineering Physics in 2002 from the Hong Kong Polytechnic University and a PhD in Non-linear and Liquid Crystal Physics in 2007 from the University of Manchester, followed by post-doctoral appointments at the Hong Kong Baptist University, Trinity College Dublin, and the

University of Nottingham. His interests lie in the fields of statistical, nonlinear and soft matter physics, with publications on topics related to particle packing, electrostatics theory, conduction and diffusion, and crystal growth.

Table 1 A selection of references relevant to recent developments in the theory of electrostatic interactions between charged particles. The list is by no means comprehensive, but papers have been selected to demonstrate the breadth of applications. Additional reference can be found in the main text

Types of particles	Theoretical methods	Ref.
Insulating sphere – conducting plane	Image charge	13
Dielectric spheres	Multipole expansion in Legendre polynomials using spherical coordinates	14
Point charge – metallic or dielectric sphere	Image charge/DFT	15
Conducting ellipsoids	Finite element methods	16
Dielectric sphere – point charge	Multipole expansion in Legendre polynomials using spherical coordinates	17
Dielectric sphere – dielectric plane	Multipole expansion in Legendre polynomials using bispherical coordinates	18
Dielectric sphere – dielectric plane	Image charge	19
Dielectric sphere – microion (point charge)	Image charge	20
Dielectric sphere – conducting plane	Image charge	21
Dielectric spheres	Spherical harmonic expansion of surface charge density	22
Charge spheres in a plasma	Screened Coulomb interaction	23
Dielectric spheres in a dielectric medium	Multipole expansion in spherical harmonics	24
Dusty plasma	Screened monopole and dipole Coulomb interaction	25
Conducting spheres	Charge defined in terms of capacitance coefficients	26
Conducting spheres	Image charge	27
Dielectric spheres	Image charge	28
Spherical nanoparticles	Numerical minimisation of free-energy	29
Dielectric spheres	Legendre polynomial expansion in bispherical coordinates	30
Dielectric sphere – dielectric plane	Image charge	31
Dielectric sphere – dielectric plane	Steady state solution of the Poisson–Nernst–Planck equations	32

electrostatic force;¹⁰ research that has subsequently seen extensive application in the field of cloud physics. The high dielectric constant of water means that a conducting sphere solution remains effective to this date. However, the vast majority of materials from which charged particles are composed, for example, volcanic ash,^{2,3} cosmic dust grains,¹¹ printer toner,⁵ food coatings,⁶ colloids,¹² *etc.*, are not conducting and therefore require a formalism that is more universally applicable. To this end, a solution to the more difficult problem of how charged dielectric spheres interact with one another has been sought for many years.

Table 1 presents a list of some of the more recent papers covering the theory of electrostatic interactions between charged particles. As can be seen, a number of the proposed solutions to the dielectric sphere interaction problem have built on the early conducting sphere solution and used image charge theory to

describe the electrostatic interaction between spheres. However, a number of studies have also adopted a multipole approach based on a spherical coordinate system, whereby each sphere possesses a defined set of electrostatic multipoles, the sum of which describe the total interactive force or energy. An advantage of this approach is that it can provide a physical picture of the extent to which the surface charge on both spheres is polarised through a mutual interaction. When reduced to a point charge – charged sphere configuration, these theories can provide the classical electrostatic multipole terms, *i.e.* ion-induced dipole, ion-induced quadrupole *etc.* Very recently, a bispherical rather than spherical coordinate system has been used to describe the electrostatic interaction between a charged dielectric sphere and a planar dielectric surface.¹⁸ This new approach has universal appeal in that it can move smoothly between the solution for a pair of finite-sized particles and a pair of planar surfaces (see below),



Anthony J. Stace

The PhD and postdoctoral research of Tony Stace focused on the development of computer models to simulate elementary chemical reactions. In 1977 the award of a SERC Advanced Fellowship enabled him to construct experiments to study the properties of clusters. In 1984 he was appointed as lecturer at Sussex, becoming a Professor in 1993. He was elected a Fellow of the Royal Society in 2002 and in 2004 he moved to Nottingham University as

Professor of Physical Chemistry. Recently he dismantled and/or gave away all of his experimental equipment and has returned to the (very much cheaper!) pleasures of computer simulation.



Elena Besley

Elena Besley is Professor of Theoretical and Computational Chemistry at the University of Nottingham, UK. Her research interests include the development of theoretical and computational approaches to prediction of materials properties; electrostatic interactions at the nanoscale; gas storage and fundamental interactions in porous solids. Elena is a recipient of the EPSRC Career Acceleration Fellowship (2008–2014), New

Directions for EPSRC Research Leaders Award (2012–2014), and ERC Consolidator Grant (2013–2017).

but has the disadvantage of being slower to converge than the spherical coordinate solution.

For many particulate systems, the particles involved all carry the same sign of charge, and one of the most interesting results to emerge from electrostatic calculations is that, under certain circumstances, like-charged particles can be attracted to one another;³³ indeed, charge scavenging processes taking place in, for example, clouds and power stations depend on such a phenomenon.^{1,7} In this perspective article, we outline some of the recent developments associated with calculating the electrostatic properties of charged dielectric spheres and in particular we examine the circumstances under which like-charged particles of dielectric materials can experience an attractive interaction. Due consideration is given to the numerical accuracy of the multipole approach adopted in some more recent solutions and also to the importance of establishing convergence criteria when addressing problems where the dielectric constants are moderately large.

1. Overview of theory

In 2010 a new theoretical model was proposed for calculating the electrostatic force between charged spheres composed from a dielectric material.¹⁴ The model describes the electrostatic interaction between a pair of spheres, with net charges q_1 and q_2 (contributed solely from the presence of free charge on the surface of each sphere), with radii a_1 and a_2 , and dielectric constants k_1 and k_2 , respectively. The spheres are assumed to be electrically non-conducting, where electrical conductivity is defined as the product of carrier mobility and charge density. Therefore, the non-conducting case implies either the absence of free charge in the system or, if free charge is present, no mobility for the free charge carriers. For a homogeneous polarisable material with a bulk polarisability described by the dielectric constant, Gauss' law states that the volume densities of free charge, polarisation charge, and total charge (the sum of free and polarisation charge) are proportional. At the surface of a dielectric sphere, the density of free and total charge can be described by a set of field discontinuities with boundary conditions, which involve dielectric constants from both sides of the surface. For a charged dielectric particle, it is assumed that the free charge is uniformly distributed on the surface, which corresponds to the lowest-energy configuration, and remains immobile during interaction; the latter assumption is justified by the zero mobility of free carriers. This condition also implies an absence of free charge inside the particle, so that only charge on the surface needs to be considered. The total surface charge density σ on a particle can be written as a sum of contributions from the polarisation charge density σ_p and the free charge density σ_f , *i.e.* $\sigma = \sigma_p + \sigma_f$, where the polarisation charge varies as a function of the sphere–sphere separation.

Fig. 1 gives a geometric representation of the problem being addressed. Two dielectric spheres are suspended in vacuum, where their dimensionless dielectric constants are defined as

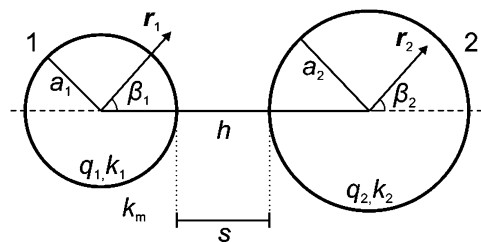


Fig. 1 A geometric representation of two charged dielectric spheres interacting in vacuum.¹⁴ Dielectric constants, charges, radii, and the polar angles of spheres 1 and 2 are denoted as k_1 , q_1 , a_1 , β_1 and k_2 , q_2 , a_2 , β_2 , respectively. The centre-to-centre separation is defined as h and the corresponding surface-to-surface separation is given by $s = h - a_1 - a_2$.

$k_i = \epsilon_i/\epsilon_0$ ($i = 1, 2$) and ϵ_0 is the permittivity of vacuum ($k_m = 1$). The charge density obeys boundary conditions that are familiar to electrostatic theory:^{34,35}

(i) Continuity of the tangential component of the electric field as a result of the continuity of the electric potential on the surface of each sphere

$$\hat{n} \times (\mathbf{E}_{r_i=a_i^+} - \mathbf{E}_{r_i=a_i^-}) = 0 \quad (1)$$

(ii) Discontinuity of the normal component of the electric field due to the presence of a total charge on the surface of each sphere.

$$\hat{n} \cdot (\mathbf{E}_{r_i=a_i^+} - \mathbf{E}_{r_i=a_i^-}) = \frac{\sigma}{\epsilon_0} \quad (2)$$

(iii) Discontinuity of the normal component of the electric displacement field due to the presence of a free charge on the surface of each sphere.

$$\hat{n} \cdot (\mathbf{D}_{r_i=a_i^+} - \mathbf{D}_{r_i=a_i^-}) = \sigma_f \quad (3)$$

where \hat{n} is a unit vector perpendicular to a point of reference on the surface of a sphere, and the subscripts a_i^+ and a_i^- denote radial positions on the outside and the inside of the surface, respectively. The electric displacement field \mathbf{D} is related to the electric field \mathbf{E} as $\mathbf{D} = k_i \epsilon_0 \mathbf{E}$.

The electrostatic force due to the presence of a total charge on the surface of each sphere is calculated from a generalization of Coulomb's law for point charges and is given by

$$\mathbf{F}_{12} = K \int dq_1(\mathbf{r}_1) \int dq_2(\mathbf{r}_2) \frac{\mathbf{r}_1 - \mathbf{r}_2}{|\mathbf{r}_1 - \mathbf{r}_2|^3} \quad (4)$$

where \mathbf{r}_1 and \mathbf{r}_2 are position vectors at the surface (as shown in Fig. 1), $dq_1(\mathbf{r}_1)$ and $dq_2(\mathbf{r}_2)$ are the corresponding charge elements, and K is Coulomb's constant. The first integral in eqn (4) takes into account the charge residing on sphere 1 and the second integral is the potential generated by the charge residing on sphere 2. The electrostatic force, \mathbf{F}_{12} , is then evaluated through a Legendre polynomial expansion of the electric potential generated by the two spheres as they interact.¹⁴ The total surface charge distribution is determined as a function of the centre-to-centre separation, h and an integration of the charge across the surface yields the following

analytical expression for the electrostatic force (further details can be found in ref. 14)

$$F_{12} = -\frac{1}{K} \sum_{l=0}^{\infty} A_{1,l} A_{1,l+1} \frac{(k_1 + 1)(l + 1) + 1}{(k_1 - 1)a_1^{2l+3}} \quad (5)$$

The convention adopted has F_{12} as negative for an attractive interaction and positive for a repulsive interaction. Dependence of the electrostatic force on the separation h is accounted for by the multipole moment coefficients $A_{1,l}$, which describe the mutual polarisation experienced by the interacting spheres as a function of their dielectric constants (k_1 and k_2), charges (q_1 and q_2) and radii (a_1 and a_2). Equations describing the multipole moments are given by

$$4\pi K a_1 \sigma_{f,1} \delta_{l,0} = \frac{A_{1,l}}{a_1^{l+1}} + \frac{(k_1 - 1)l}{(k_1 + 1)l + 1} \sum_{m=0}^{\infty} A_{2,m} \frac{(l + m)!}{l!m!} \frac{a_1^l}{h^{l+m+1}} \quad (6)$$

and

$$4\pi K a_2 \sigma_{f,2} \delta_{l,0} = \frac{A_{2,l}}{a_2^{l+1}} + \frac{(k_2 - 1)l}{(k_2 + 1)l + 1} \sum_{m=0}^{\infty} A_{1,m} \frac{(l + m)!}{l!m!} \frac{a_2^l}{h^{l+m+1}} \quad (7)$$

for sphere 1 and 2, respectively. After eliminating $A_{2,l}$, eqn (6) and (7) and can be combined to yield A_{1,j_1}

$$A_{1,j_1} = a_1 V_1 \delta_{j_1,0} - \frac{(k_1 - 1)j_1}{(k_1 + 1)j_1 + 1} \frac{a_1^{2j_1+1}}{h^{j_1+1}} a_2 V_2 + \frac{(k_1 - 1)j_1}{(k_1 + 1)j_1 + 1} \times \sum_{j_2=0}^{\infty} \sum_{j_3=0}^{\infty} \frac{(k_2 - 1)j_2}{(k_2 + 1)j_2 + 1} \frac{(j_1 + j_2)! (j_2 + j_3)!}{j_1! j_2! j_3!} \times \frac{a_1^{2j_1+1} a_2^{2j_2+1}}{h^{j_1+2j_2+j_3+2}} A_{1,j_3} \quad (8)$$

where $a_1 V_1 = K q_1$ and $a_2 V_2 = K q_2$. Taking into account the fact that $A_{1,0} = 4\pi K a_1^2 \sigma_{f,1}$ and $A_{2,0} = 4\pi K a_2^2 \sigma_{f,2}$, the electrostatic force can be written as

$$F_{12} = K \frac{q_1 q_2}{h^2} - q_1 \sum_{m=1}^{\infty} \sum_{l=0}^{\infty} A_{1,l} \frac{(k_2 - 1)m(m + 1)}{(k_2 + 1)m + 1} \times \frac{(l + m)!}{l!m!} \frac{a_2^{2m+1}}{h^{2m+l+3}} - \frac{1}{K} \sum_{l=1}^{\infty} A_{1,l} A_{1,l+1} \frac{(k_1 + 1)(l + 1) + 1}{(k_1 - 1)a_1^{2l+3}} \quad (9)$$

Eqn (9) gives a simple and well-behaved solution for the electrostatic force between two charged polarisable spheres as a function of their separation, h . The first term in the equation is the Coulomb force between two non-polarisable spheres or point charges, separated by a distance h . The second and third terms in eqn (9) account for the contribution polarisation makes to the overall electrostatic force; these terms are always negative and represent an attraction between the spheres that increases in magnitude as a function of dielectric constant. The effect of these attractive contributions is to diminish the magnitude of the repulsive Coulomb force, and for certain

combinations of q_i , a_i and k_i , like-charged spheres can become attracted to one another at short separation. In the limit $l = 0$, the first and second terms in eqn (9) represent the electrostatic force between a charged polarisable sphere and a non-polarisable sphere (or a point charge), and if taken a step further with $q_2 = 0$, we obtain a well-known classical electrostatic solution for describing the attraction between a neutral polarisable sphere and a point charge.^{34,35}

Although the spherical coordinate solution outlined above has proved very successful at accounting for a wide range of experimental data involving pairs of charged particles,^{36–38} the formalism has been found not to be suitable for applications to particle–planar surface interactions. To this end, a new solution using bispherical coordinates to describe the electrostatic interaction between a dielectric, charged particle and a planar dielectric surface was proposed in 2014.¹⁸ This approach has proved to be applicable to charged particles of all dimensions, but does converge more slowly than the spherical coordinate solution (see below).

2. Like-charge attraction

2.1 Origin

The attraction between like-charged dielectric particles arises from a mutual polarisation of surface charge for certain combinations of radius, charge, and dielectric constant.³³ Fig. 2 shows graphically an example where a specific combination of charge and radii can result in an attractive interaction. Qualitatively, the interaction can be divided into two regions: a long-range repulsion that is equivalent to the Coulomb force experienced by two non-polarisable spheres or point charges, described by the first term in eqn (9), and a dominant short-range attraction due to mutual polarisation of the spheres, where the second and third terms of eqn (9) prevail.

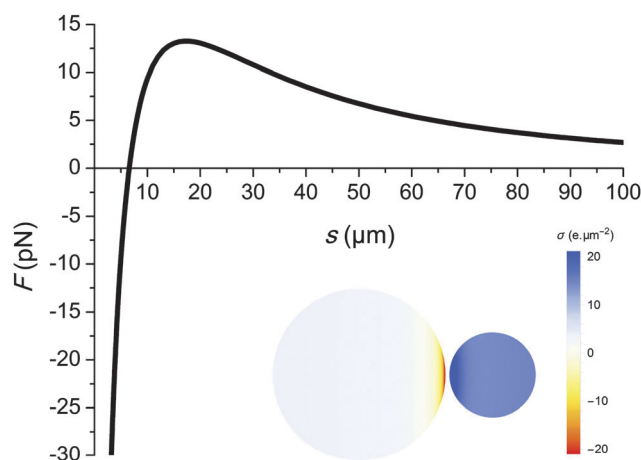


Fig. 2 The electrostatic force as a function of the surface-to-surface separation between two spheres with $k_1 = k_2 = 20$, $a_1 = 20 \mu\text{m}$, $a_2 = 10 \mu\text{m}$, $q_1 = 10 \times 10^3 e$ and $q_2 = 20 \times 10^3 e$ calculated using eqn (9). Also shown is a charge density map plotted on the surface of each sphere at $s = 1 \mu\text{m}$, ($s = h - a_1 - a_2$).

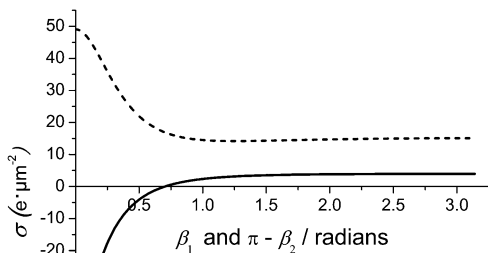


Fig. 3 The total surface charge density as a function of the polar angle calculated for the pair of spheres shown in Fig. 2 at a surface-to-surface separation of $s = 1 \mu\text{m}$. The charge density on sphere 1 is shown by solid line and on sphere 2 by dashed line.

For the conditions specified in Fig. 2, a calculation has been made of the surface charge density as a function of the polar angle β_i (Fig. 1). A qualitative picture of how the charge is distributed across the surface of each sphere is shown in Fig. 2 and more detail is given in Fig. 3. Together these results illustrate how the interaction between two like-charged particles can lead to a net attraction when the particles are in close proximity. As can be seen, the greater surface charge density on the smaller of the two spheres induces an area of negative charge on the larger sphere in a region close to the point of contact ($\beta_2 = \pi - \beta_1 \rightarrow 0$). In turn, the latter induces an area of enhanced positive charge on the smaller sphere that is again close to the point of contact. The net effect is that, at very short sphere–sphere separations, the attraction between these two regions of opposite charge is stronger than any Coulomb repulsion between the permanent free charges. However, this effect only becomes significant at short separation, and as Fig. 2 shows, attraction is rapidly replaced by repulsion as s increases.

Materials where a value of $k_i = 20$ might be appropriate include, for example, liquid droplets composed of compounds that contain either nitrogen or oxygen atoms, *e.g.* ammonia or methanol. It should be noted, however, that the dielectric constant typically describes the extent to which a bulk material concentrates electric flux, and when used in the context of a very small particle, it may lose that significance and instead take the form of a parameter, which reflects the polarisability of a particle.

2.2 The effects of size, charge and dielectric constant of the interacting particles

This section presents a more detailed investigation into the conditions under which like-charge attraction occurs and further analysis of the physical significance of this counter-intuitive phenomenon is given. To explore the consequences of treating spheres as being composed of dielectric materials, we present a series of calculations that examine changes in the strength of like-charge attraction depending on both the dielectric constants and separation between the spheres.

Increasing k_i should increase the contribution that polarisability makes towards diminishing the effects of Coulomb repulsion between the spheres. For $k_1 = k_2 = 1000$, the spheres are assumed to be approaching the metallic limit. As Fig. 2 would suggest, changing the separation between spheres can alter the balance between contributions to the force from long-range Coulomb repulsion and short-range attractive polarisation. For six different values of $k_1 = k_2$, the magnitude of the electrostatic force has been determined as a function of charge ratio q_2/q_1 ranging from 0 to 10 and radius ratio a_2/a_1 also ranging from 0 to 10. These results are plotted in Fig. 4. For the purpose of comparison, analytical zero force curves obtained from Lekner's model,²⁶ which describes interactions between conducting spheres, are presented as light blue lines in Fig. 4. Analytical zero force curves are calculated from the point on the curve in Fig. 2 where Coulomb repulsion is cancelled out by attractive polarisation interactions. As it can be seen, Lekner's model agrees almost exactly with results calculated from the dielectric sphere model with $k_i = 1000$. Broadly speaking each of the diagrams shown in Fig. 4 can be divided into three regions: (i) when $a_2 \gg a_1$ the scale of the attractive interaction is dominated by the ability of the high charge density on the smaller particle to polarise the larger particle; this can be achieved even under circumstances where the charge ratio q_2/q_1 is also increasing; (ii) as the ratio a_2/a_1 decreases, the contribution polarisation makes to the interaction diminishes and the force between particles becomes dominated by Coulomb repulsion; (iii) as a_2/a_1 decreases still further, particle polarisation again begins to dominate the strength of the interaction, particularly as the ratio q_2/q_1 increases. For dielectric particles of any composition, this latter combination of a_2/a_1 and q_2/q_1 would appear to provide the most favourable conditions for a strong attractive interaction. As Fig. 4 shows, the dielectric response of each sphere makes a significant contribution to the nature of the mutual interaction they experience in close proximity. Even particles composed of weakly polarisable materials ($k_i = 2$, Fig. 4a), for example oils, plastics, and dust, can be attracted to one another at certain values of size and/or charge ratio; large differences in charge can lead to a particularly strong attraction. As the dielectric constant increases towards a value appropriate for water droplets,¹ a very significant fraction of the contour plot denotes the presence of an attractive interaction between spheres.

The next few examples show how the degree of attraction between like-charged spheres varies as a function of their separation. For six values of the surface-to-surface separation s , the magnitude of the electrostatic force has been determined as a function of the q_2/q_1 and a_2/a_1 ratio ranging from 0 to 10. These results are plotted in Fig. 5. To better illustrate the effect of polarisation, and consequently the attractive component of the force, the dielectric constants have been fixed at a value of $k_1 = k_2 = 1000$. Analytical zero force curves (in blue) obtained from Lekner's model for conducting spheres are also included.²⁶

As the results show, there are clearly defined circumstances where like-charged particles are attracted to one another,

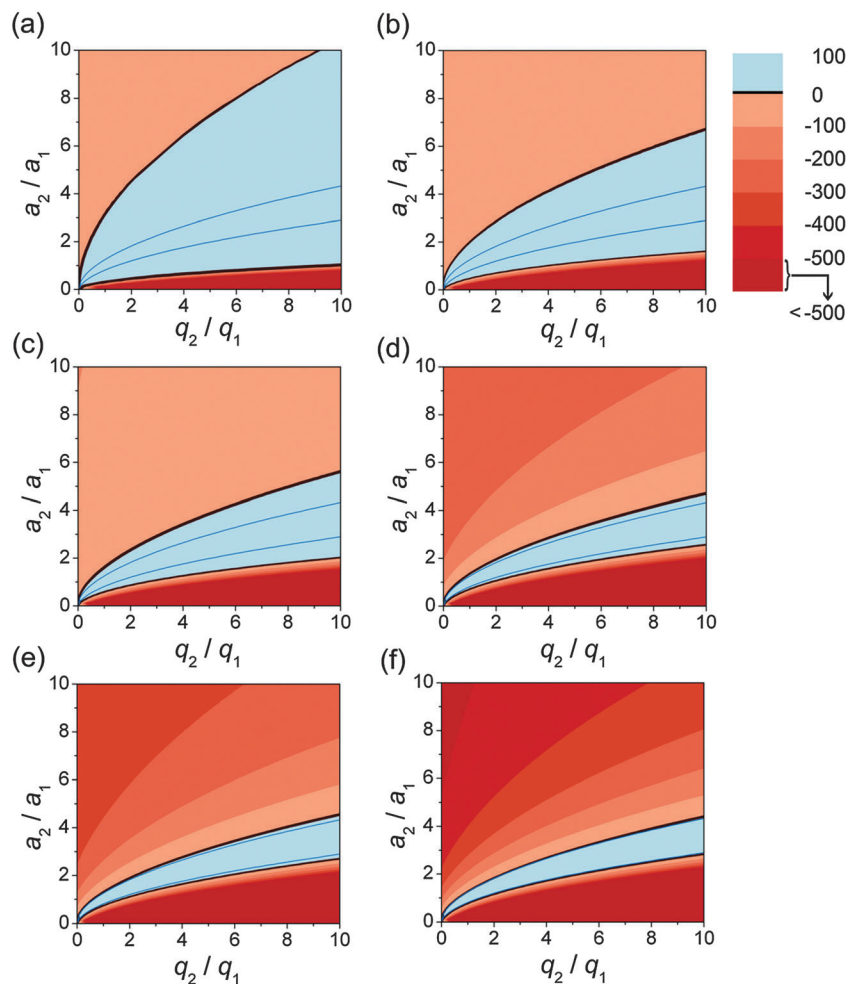


Fig. 4 Contour maps of the electrostatic force (in pN) as a function of the charge ratio q_2/q_1 and radius ratio a_2/a_1 , for a pair of like-charged spheres separated by a fixed distance of $s = 0.01 \mu\text{m}$ and with different values of the dielectric constant: $k_1 = k_2 = 2$ (a), 5 (b), 10 (c), 40 (d), 80 (e) and 1000 (f). The radius of sphere 1 is fixed at $a_1 = 1 \mu\text{m}$ and charge at $q_1 = 1 \times 10^3 e$. As the dielectric constant decreases the electrostatic force can change from attractive to repulsive as it shifts towards the Coulomb limit of two non-polarisable spheres. The convention is that a negative force denotes a net attraction between the particles.

even when the separations involved are comparable to their size. For example, particles separated by $1 \mu\text{m}$ could coalesce if they carry the same amount of charge, but have a radii ratio of 4:1. Both Fig. 4 and 5 show that the attraction between particles can become markedly stronger if there is a large disparity in the amount of charge they carry. The latter effect becomes amplified when it is also accompanied by an increase in the value of the dielectric constant for the interacting spheres. It is interesting to note that the results in Fig. 5a would suggest that particles of radius $1 \mu\text{m}$ and $10 \mu\text{m}$, both composed of a high dielectric material and carrying a similar amount of charge, would be attracted to one another over a distance of $5 \mu\text{m}$. Since these effects scale up it is easy to see how physical processes, such as charge scavenging,^{1,7} can operate quite readily under conditions where one of the particles may have a radius of $1 \mu\text{m}$ or more. Fig. 4 and 5 serve as replacements for an equivalent plot given in ref. 14 as these earlier calculations did not take into account all the polarisation terms necessary to obtain fully converged values of the force

(see below). The good agreement between Lekner's model for conducting spheres and the dielectric model with $k_i = 1000$ suggests that results from the latter converge to the correct limit when the theory is applied to particles with very large dielectric constants.

As shown in Fig. 4 and 5, the repulsive region always passes through a point corresponding to $a_2/a_1 = 1$ and $q_2/q_1 = 1$, *i.e.* for identical spheres. Since such spheres have equivalent electrostatic properties, there exists a balance between the mutual repulsive and polarising effects they exert on one other, and as a result the spheres present mirror-symmetric surface charge distributions, as illustrated in Fig. 6.

The mutual polarisation experienced by two identical interacting spheres results in regions of negative and positive polarisation surface charge. However, as Fig. 6b shows, the total surface charge density, $\sigma_p + \sigma_r$, is positive everywhere on the surface of the spheres, and therefore the overall force between the particles is repulsive. In this particular case, polarisation effects merely serve to weaken the Coulomb repulsion that arises from the presence of

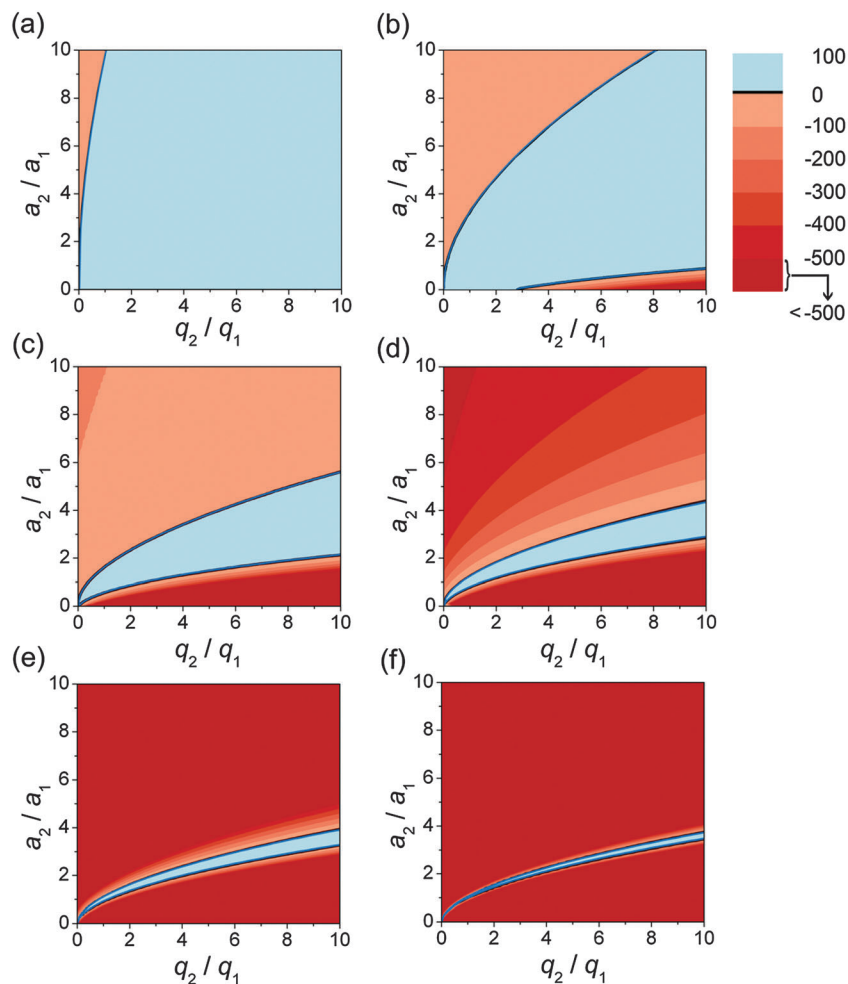


Fig. 5 Contour maps of the electrostatic force (in pN) as a function of the charge ratio q_2/q_1 and radius ratio a_2/a_1 , for a pair of like-charged spheres at various surface-to-surface separations: $s = 5 \mu\text{m}$ (a), $1 \mu\text{m}$ (b), $0.1 \mu\text{m}$ (c), $0.01 \mu\text{m}$ (d), $0.001 \mu\text{m}$ (e) and $0.0001 \mu\text{m}$ (f). The value of the dielectric constant is $k_1 = k_2 = 1000$. The radius of sphere 1 is fixed at $a_1 = 1 \mu\text{m}$ and charge at $q_1 = 1 \times 10^3 e$.

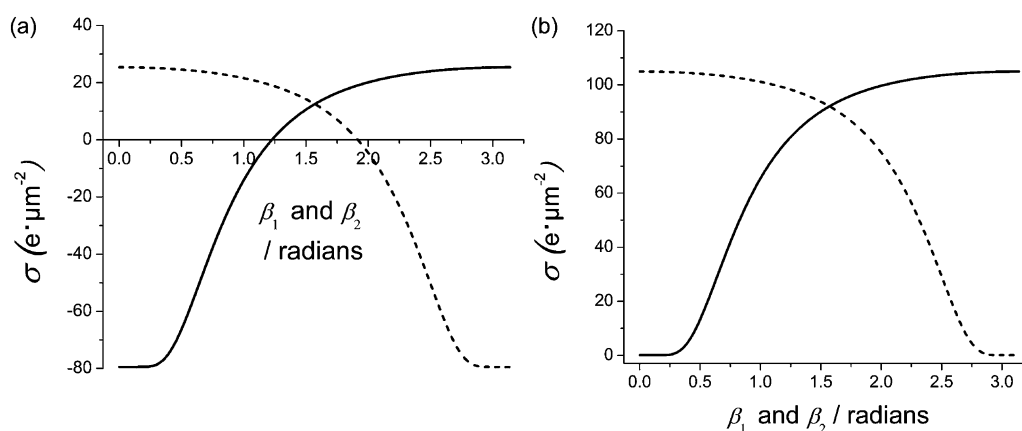


Fig. 6 Polarisation surface charge density (a) and total surface charge density (b) as a function of the polar angle calculated for a pair of identical spheres with $k_1 = k_2 = 1000$, $a_1 = a_2 = 1 \mu\text{m}$, and $q_1 = q_2 = 1 \times 10^3 e$ separated by $s = 0.01 \mu\text{m}$. The charge density on sphere 1 is shown by solid line and on sphere 2 by dashed line.

free charge, and so the net electrostatic force is weaker than it would be for the same pair of identical spheres but with $k_1 = k_2 = 1$,

i.e. for non-polarisable spheres, or equivalently for two point-charges with $q_1 = q_2 = 1 \times 10^3 e$ and separated by $0.01 \mu\text{m}$.

3. Electrostatic force with respect to system geometry

Much of the research carried out on pair interactions in the field of electrostatics describes the interacting body as a point particle, a sphere or a plane. The exact geometry of a system consisting of a pair of such interacting objects is dependent upon length scales, namely on the radii of the particles and their surface-to-surface separation. For example, if the separation between two spheres is much larger than their radii, the system approaches the geometric limit of two point particles. A systematic approach to transformations in length scale has recently been proposed in the form of a general geometric representation based on the bispherical coordinate system introduced earlier.^{18,39} The formalism introduces a dimensionless, scaled surface-to-surface separation parameter $s^* = s/2a$, where s is the surface-to-surface separation and $2a$ is the distance between the two inverse points in the bispherical coordinate system.^{39,40} For a two-body problem, this approach makes possible a description covering all possible combinations of

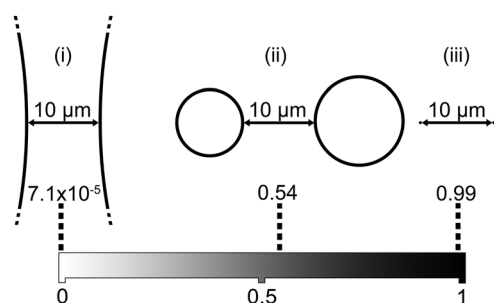


Fig. 7 A geometric representation of two spheres separated by the surface-to-surface separation of $s = 10 \mu\text{m}$: (i) $a_1 = a_2 = 500 \mu\text{m}$ (ii) $a_1 = 5 \mu\text{m}$, $a_2 = 7.5 \mu\text{m}$ (iii) $a_1 = a_2 = 0.05 \mu\text{m}$ (iii). The scaled surface-to-surface separation parameter s^* ranges from 0 to 1 and is shown as a continuum of the values corresponding to all possible combinations of sphere size and separation distance (adapted from ref. 39).

sphere size and surface-to-surface separation.³⁹ The scaled surface-to-surface separation parameter approaches the limit $s^* = 1$ if the radii of both spheres are much smaller than the actual surface-to-surface distance s , *i.e.* in the limit of two point particles. At the other extreme, the geometric limit of $s^* = 0$ corresponds to either two planar surfaces or two interacting spheres with radii that are very much larger than s . Fig. 7 provides a geometric description of how s^* transforms according to the physical nature of the interacting bodies.

For any given charge ratio q_2/q_1 , the electrostatic force can now be studied as a function of s^* with respect to any given geometric configuration. As an example, consider a pair of like-charged spheres with radius $a_1 = a_2 = 1 \mu\text{m}$. Let the free charge on sphere 1 be fixed at $q_1 = 1 \times 10^3 e$ such that the free charge on sphere 2 and the surface-to-surface separation account for the only two variables in the system, which can be expressed as the charge ratio q_2/q_1 and the scaled surface-to-surface separation s^* . Fig. 8 shows how the electrostatic force depends on these two parameters, for two cases: (a) $k_1 = k_2 = 1000$; and (b) $k_1 = k_2 = 10$. For (a), at the limit $s^* = 0$, which can correspond to either two planar surfaces or two large spheres in very close proximity, the repulsive force vanishes completely apart from when $q_2/q_1 \rightarrow 1$; as the charge ratio approaches unity from either direction, the magnitude of the repulsive Coulomb term (see eqn (9)) increases gradually until it balances the attractive polarisation terms of the force. However, under all circumstances other than $q_2/q_1 \rightarrow 1$, two like-charged equal-sized spheres at the limit of $s^* = 0$ will always be attracted to one another if they are of metallic nature. This result is consistent with Lekner's²⁶ conclusion regarding the behaviour of charged metallic spheres in close proximity. One can note a marked difference at the limit of $s^* \rightarrow 0$ for case (b), where the particles have considerably smaller dielectric constants and are therefore less polarisable. The range of q_2/q_1 values over which the particles will repel each other is much larger than for case (a) and overall, the attractive polarisation contributions to the force are smaller, which means that the region of repulsion is

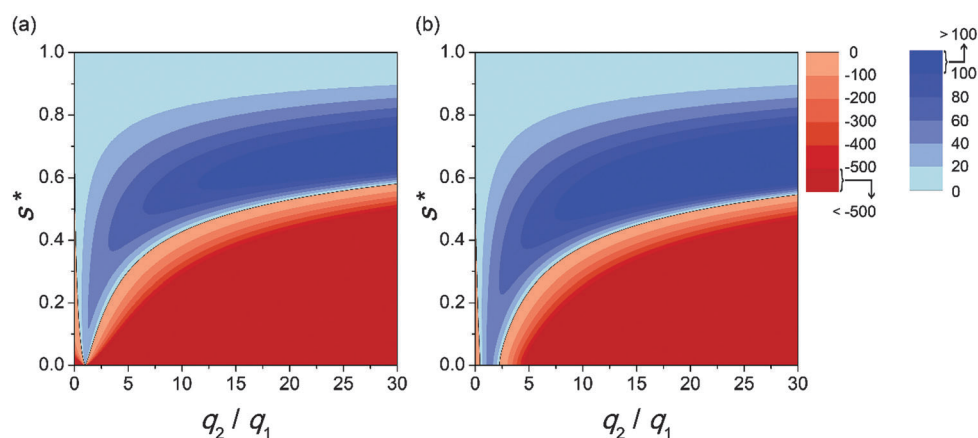


Fig. 8 Contour map of the electrostatic force (in pN) between a pair of equal-sized, like-charged spheres, with dielectric constants (a) $k_1 = k_2 = 1000$ and (b) $k_1 = k_2 = 10$. The force is plotted as a function of the scaled surface-to-surface separation s^* ³⁹ and the charge ratio q_2/q_1 , with $a_1 = a_2 = 1 \mu\text{m}$ and $q_1 = 1 \times 10^3 e$. The regions of attractive and repulsive forces are separated by a thin black solid line, which denotes the cases of zero force.

more pronounced. At the other geometric limit $s^* = 1$ for two point particles, the attractive contributions to the total force become increasingly less significant and at some point are overtaken by a more pronounced repulsive Coulomb component. Consequently, the forces in both case (a) and (b) are dominated by the Coulomb term for two point charges and the corresponding contour plots become very similar.

Numerical calculations show that, if the radii of two spheres and their separation are all multiplied by an arbitrary factor α , the electrostatic force will change by a factor of $1/\alpha^2$. This is illustrated in Fig. 9a and b for plots of the electrostatic force as a function of the radius ratio a_2/a_1 , and where the force is shown to have decreased by a factor of 1/100 as the various length quantities are increased by a factor of 10. Conversely, if the charges q_1 and q_2 on two spheres are both multiplied by α , the electrostatic force will change by a factor of α^2 . Fig. 10a and b show how the force as a function of the charge ratio q_2/q_1 increases by a factor of 100 when q_1 and q_2 are both multiplied by a factor of 10. These observations suggest a certain degree of generality of the results, in the sense that values for the force can be scaled up or down to any desired order of magnitude. For example, in the results presented in this paper the values of force, length (radii and separation distances) and charge are given respectively in units of piconewton, micrometer and

orders of $10^3 e$; however, contour maps that are equivalent to those shown in Fig. 4, 5 and 8 can be generated to give micro-newton forces between particles, with radii and separation distances in the millimeter range and charges of orders of $10^9 e$.

4. Convergence rates

Since the electrostatic force given by eqn (9) is represented as a sum of multipole moments, it is instructive to examine how rapidly the series converges. In a number of applications, particularly when used in conjunction with water droplets, the equivalent point charge – sphere series expansion is often truncated after the first two terms.¹ The convergence tests also provide an opportunity to examine differences between the two solutions presented using either spherical polar or bispherical coordinates.^{14,18} Fig. 11 shows the results of calculations, where the number of terms in the multipole expansion required to achieve a precision of ten significant figures in the calculated electrostatic force has been explored in terms of three variables: surface-to-surface separation, s ; radius ratio, a_2/a_1 ; and dielectric constant, $k_1 = k_2$. The influence of the charge ratio q_2/q_1 is considered separately in Fig. 12. Since the effects of polarisation are manifested through the multipole terms in eqn (9), the results

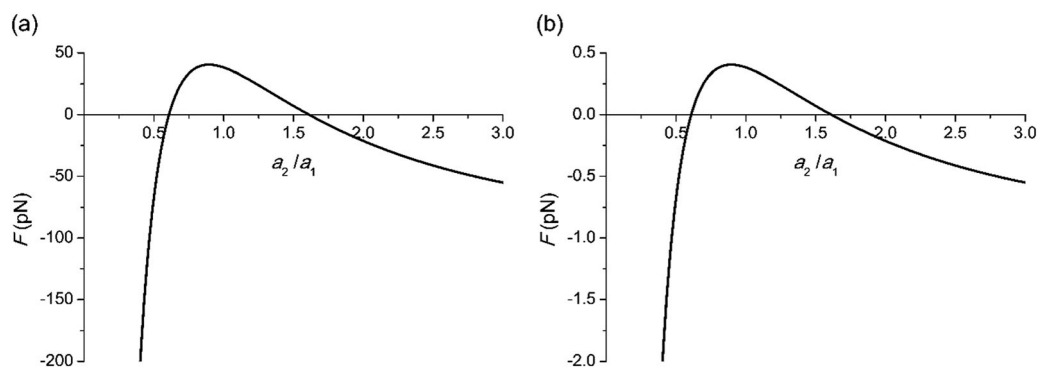


Fig. 9 Plots of the electrostatic force (pN) as a function of the radius ratio a_2/a_1 . The dielectric constants and charges of the spheres are given by $k_1 = k_2 = 10$ and $q_1 = q_2 = 1 \times 10^3 e$, respectively. For (a), the radius of sphere 1 and the surface-to-surface separation are fixed at $a_1 = 1 \mu\text{m}$ and $s = 0.01 \mu\text{m}$, while the values of these two parameters in (b) are greater by a factor of 10. The force values in (b) are therefore a hundred times less than those in (a).

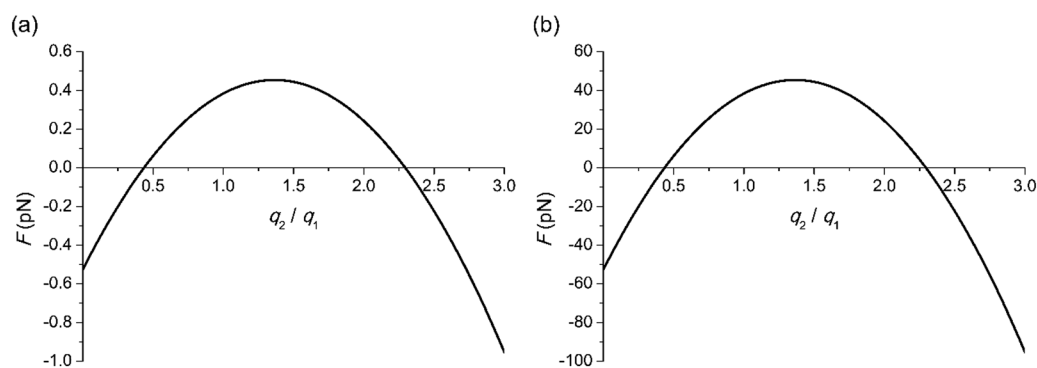


Fig. 10 Plots of the electrostatic force (pN) as a function of the charge ratio q_2/q_1 . The dielectric constants, radii of the spheres as well as their surface-to-surface separation are given by $k_1 = k_2 = 10$, $a_1 = a_2 = 10 \mu\text{m}$, and $s = 0.01 \mu\text{m}$, respectively. The charge of sphere 1 is fixed at $q_1 = 1 \times 10^3 e$ and $q_1 = 10 \times 10^3 e$ for (a) and (b), respectively. The force values in (b) are therefore a hundred times greater than those in (a).

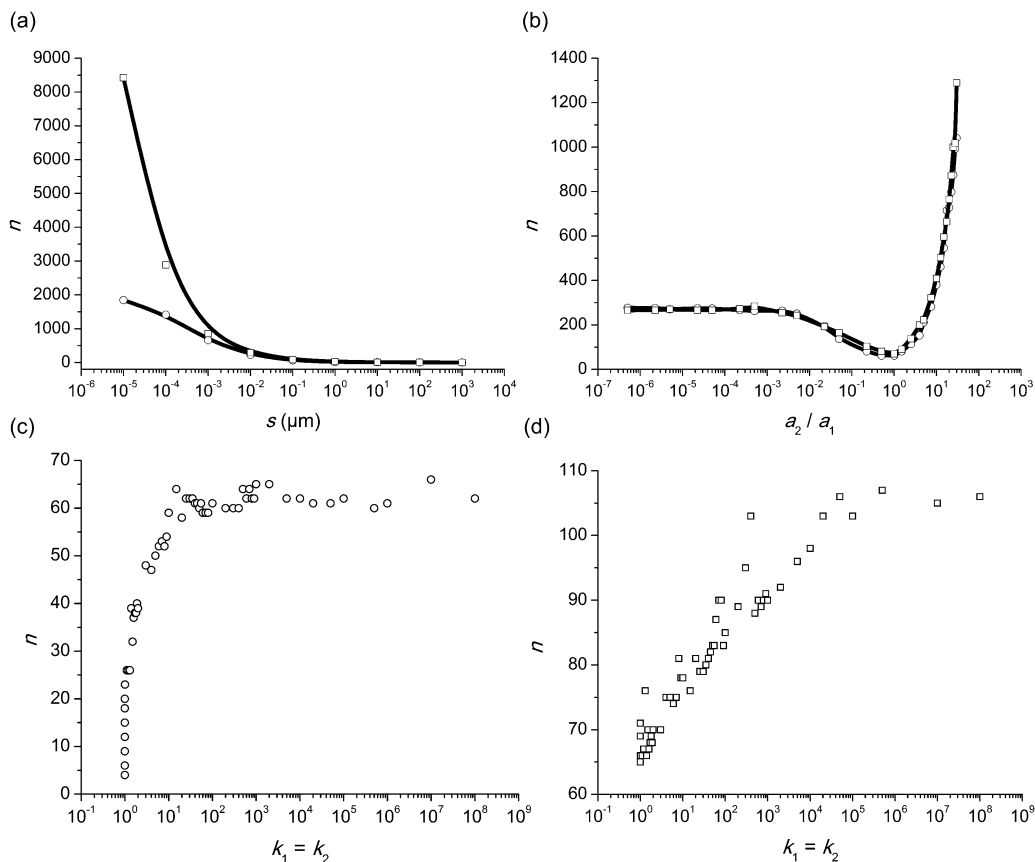


Fig. 11 Comparison of the convergence conditions for the electrostatic force, obtained using the spherical polar (\circ)¹⁴ and bispherical (\square)¹⁸ solutions, between two charged dielectric particles with $k_1 = k_2 = 40$, $a_1 = 2 \mu\text{m}$, $a_2 = 1 \mu\text{m}$, $q_1 = 2 \times 10^3 e$, $q_2 = 1 \times 10^3 e$, $s = 0.1 \mu\text{m}$: semi-log plots of the dependence of the number of terms in the multipole expansion (9) on the surface-to-surface separation (a); on the radius ratio (b); and on the dielectric constant (c) and (d).

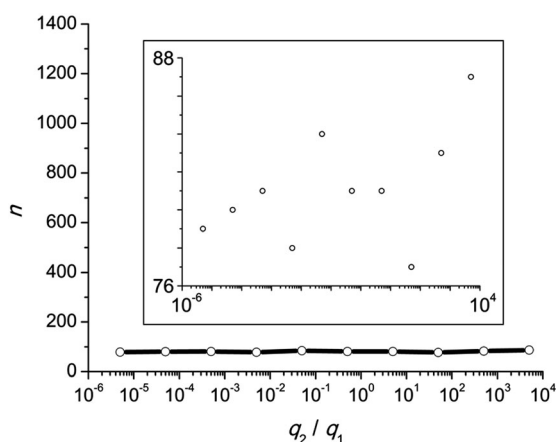


Fig. 12 Semi-log plot of the dependence of the number of terms in the multipole expansion on the charge ratio, q_2/q_1 . The inset shows an expanded y-axis. The remaining parameters were assigned the following values: $k_1 = k_2 = 40$, $a_1 = 2 \mu\text{m}$, $a_2 = 1 \mu\text{m}$, $q_1 = 2 \times 10^3 e$, $s = 0.1 \mu\text{m}$. Only data points taken from the bispherical solution are shown.

in Fig. 4 and 5 would suggest that considerable differences might be expected in the number of terms required to achieve convergence when the ratios of particle size and charge are

different from unity and/or when there are variations in particle-particle separation. Fig. 11a shows how convergence depends on the particle-particle separation, and as might be expected, the result reflects the distance-dependences of the multipolar terms that appear in the series expansion and vary as a combination of inverse powers of $h = a_1 + a_2 + s$ (eqn (9)). The first few multipole terms contributing to the force are monopolar, dipolar, and quadrupolar in nature, and at sufficiently large distances, namely where the system is close to the limit of two point charges, Fig. 11a would imply that only the monopole term prevails (also see Fig. 2). However, as the particle-particle separation decreases there is a very evident and rapid increase in the number of terms required to achieve convergence. In some respects, the number of terms in the expansion can be considered as an indirect measure of the level of induced polarisation taking place between two interacting spheres. At very large values of s there is virtually no polarisation and therefore a minimum number of terms is required; however, close to the touching limit of $s = 0$ the degree of induced polarisation is very high. As can also be seen, for small values of s , the spherical polar solution converges with fewer terms than the bispherical solution.

Fig. 11b shows how convergence of the multipole series depends on the radius ratio a_2/a_1 , and to simplify the problem,

the geometric variables a_1 and s have been fixed and only a_2 has been allowed to vary. As can be seen, the number of terms required to achieve convergence increases as the ratio a_2/a_1 moves away from unity in either direction; however, for $a_2/a_1 > 1$ there is a particularly dramatic increase seen in the number of terms required. As in the above discussion for Fig. 4, the occurrence of like-charge attraction is conditional upon either one sphere being large and very polarisable or being very small and carrying a much higher free charge. In the situation where $a_2/a_1 \sim 1$, neither of these conditions is met, and therefore the number of terms required to describe the effects of polarisation reaches a minimum. With a progressive decrease in a_2 the system begins to resemble the point-charge – sphere case, where mutual polarisation no longer occurs and the number of terms needed to account for the behaviour of (a fixed radius) sphere 1 rapidly reaches an upper limit. In contrast, a progressive increase in the radius of sphere 2, such that $a_2/a_1 > 1$, moves the system towards the planar surface – sphere limit. Hence, as a_2 increases (whilst maintaining fixed values for a_1 and s) the polarisable volume available within sphere 2 increases rapidly, and this is reflected in the number of terms required to achieve convergence.

A particle in an external electric field has a polarisability that is proportional to $(k_i - 1)$, and for larger values of the dielectric constant k_i , a particle will have a greater degree of freedom to counterbalance an external electric field and so minimize the system's electrostatic energy by means of an induced polarisation charge. At the limit of infinite k_i , a particle will enjoy complete freedom to polarise itself to achieve energy minimization. This is analogous to the case of a charged metallic sphere, where the charge is free to redistribute instantaneously in an electric field to achieve energy minimization. Zettergren *et al.* have shown theoretically¹⁵ that a charged sphere of infinite dielectric constant will achieve the same lowest-energy charge distribution as a charged metallic sphere, if they are placed in the neighborhood of a point charge. Fig. 11c and d show the behaviour of the two mathematical solutions in response to changes in the value of the dielectric constant assigned to each particle. While there is a marked difference between the two cases for relatively small values of the dielectric constant, in both cases the number of terms required for convergence approaches a constant value for increasing dielectric constant, and it eventually flattens out once the charge distribution corresponding to the lowest electrostatic energy is achieved. On the other hand, while the difference between Fig. 11c and d would imply that fewer terms are needed in the spherical polar solution to provide an accurate representation of the polarisability of a particle, from either solution it is evident that a considerable number of terms is required to provide an accurate description of the interaction between highly polarisable particles, such as two water droplets.¹ As noted earlier, although slower to converge, the strength of the bispherical solution lies in the ability to model particle–surface interactions.

Fig. 12 shows how the convergence conditions vary with the ratio q_2/q_1 , where in contrast to the previous tests shown

in Fig. 11, the number of terms in the multipole series fluctuates as the charge ratio changes. Although an increase in charge on sphere 2 does increase the degree of polarisation present on sphere 1, the conditions presented in Fig. 12 are such that polarisability of the latter is constrained by a fixed radius. Since polarisation effects depend on the size of the interacting spheres, fixed radii (limited area) imply that the level of polarisation becomes saturated, even if the spheres continuously acquire more charge. The y-axis on Fig. 12 is deliberately set to be the same as that for Fig. 11b in order to show that response of the multipole expansion to changes in q_2/q_1 is reduced significantly from that seen for changes in particle separation, radius and dielectric constant. However, there are fluctuations in the conditions necessary for series convergence and these can be seen on an expanded scale in the inset to Fig. 12. In response to changes in q_2/q_1 , there is no significant difference between the two mathematical solutions.

As a final contribution to this discussion on convergence of the multipole expansion of the electrostatic force, we examine the consequences on the calculated force of neglecting higher order terms in the expansion. Two examples are considered using the parameters presented in the inset of Fig. 13. The first example is where $k_i = 5$ and might be appropriate for an interaction between charged oil droplets, and the second example is where $k_i = 80$ and closely corresponds to conditions of water droplet size and charge that match the charge scavenging mechanism used to describe the growth of water droplets in clouds.¹ Fig. 13 shows the percentage error in the calculated force obtained by truncating the terms higher than n . For example, if a calculation of the electrostatic force between two water droplets separated by $1 \mu\text{m}$ just used the first 10 terms in the multipole expansion, then the final result would be in error by $\sim 35\%$. To maintain the same percentage error when the surface-to-surface separation is reduced to $0.1 \mu\text{m}$ it would require over 20 terms. Even for materials with a low dielectric constant, there would appear to be a need for significantly more terms than just the

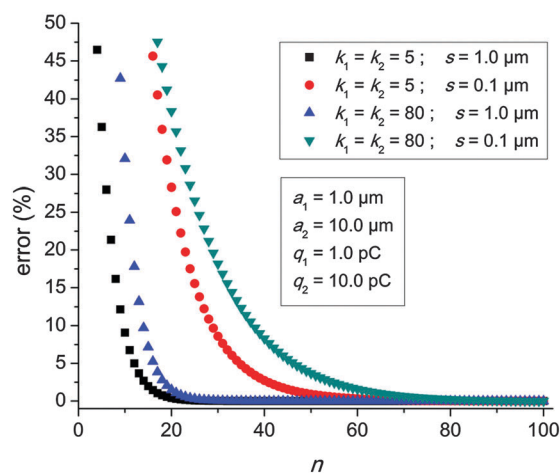


Fig. 13 Plot of the percentage error in the calculated electrostatic force with respect to the exact value (with a precision of ten significant figures) as a function of the number of terms, n in the multipole expansion (eqn (9)).

usual charge – induced dipole to give a quantitative account of a particle–particle interaction.

Conclusions

The development of a theoretical understanding of how charged particles interact with one another has a long history, which began in the 1840's with the seminal work of Kelvin on conducting spheres. However, recent advances in science and technology have demonstrated the need for a comprehensive theory that can embrace the far broader topic of dielectric particles. Within this remit are particulate materials and applications ranging from volcanic and power station ash through paints and ink jet prints and on to colloidal suspensions of tailor-made nanoparticles.

The recent contributions^{14,18} to existing solutions to the problem of electrostatic interactions between charged dielectric particles have shown excellent quantitative agreement with experimental measurements of the force between charged microspheres suspended in non-polar solvents.³⁷ Measurements of the repulsive Coulomb force between poly-methyl methacrylate spheres suspended in hexadecane, which contains a variable concentration of sodium-aerosol-OT acting as a charge control agent, is a relevant example.^{41,42} Under conditions of very low ionic strength, the agreement between experiment^{41,42} and theory¹⁴ across a large data set is excellent. The proposed theoretical solutions^{14,18} also take into account a dynamic distribution of surface charge on the interacting particles that can be displaced in response to both the strength of the electrostatic interaction and the separation distance. A net effect of the surface charge displacement is to reduce the magnitude of the electrostatic repulsion experienced by the particles with respect to that determined directly from Coulomb's law. As a result, the interacting particles are able to accommodate more charge than would be apparent from a direct fit to the Coulomb law.³⁷

With the emergence of appropriate theories has come a better understanding of the physics that is responsible for the electrostatic interactions that govern how the dielectric particles might behave. In particular, it has been shown that the forces responsible for like-charge attraction between particles depend critically on the polarisabilities of the materials involved and that, given the right circumstances, even weakly polarizable spheres, such as oil droplets, can exhibit a like-charge attraction that might be strong enough for the droplets to coalesce.

There are additional aspects of the theory that will need to be addressed in the near future. What has been outlined above holds only for particles suspended in vacuum. Whilst that is sufficient for very many applications, there are equally significant problems associated with particles held in a medium. The introduction of a medium might also need to take into account cases with the presence of an electrolyte, which charged particles may need in order to remain in suspension. Current theories covering the behaviour of charged particles in a dilute solution of an electrolyte do not support the possibility that like-charged particles may be attracted to one another. The implications of

such behaviour for electrostatically driven processes in a medium, such as self-assembly, would be of great interest from both the scientific and engineering points of view.

Acknowledgements

EBL is supported by a PhD scholarship from the Brazilian Government's Science Without Borders Programme (CAPES: 0702/13-7). EB acknowledges an ERC Consolidator Grant for financial support.

References

- 1 B. A. Tinsley, *Rep. Prog. Phys.*, 2008, **71**, 066801.
- 2 T. A. Mather and R. G. Harrison, *Surveys in Geophysics*, 2006, **27**, 387–432.
- 3 R. G. Harrison, K. A. Nicoll, Z. Ulanowski and T. A. Mather, *Environ. Res. Lett.*, 2010, **5**, 024004.
- 4 X. Meng, J. Zhu and J. Zhang, *J. Phys. D: Appl. Phys.*, 2009, **42**, 065201.
- 5 H. Jiang and L. Lu, *Atmos. Environ.*, 2010, **44**, 3347–3351.
- 6 M. K. I. Khan, M. A. I. Schutyser, K. Schroën and R. M. Boom, *J. Food Eng.*, 2012, **111**, 1–5.
- 7 A. Jaworek, A. Krupa and T. Czech, *J. Electrostat.*, 2007, **65**, 133–155.
- 8 M. K. Mazumder, R. A. Sims, A. S. Biris, P. K. Srirama, D. Saini, C. U. Yurteri, S. Trigwell, S. De and R. Sharma, *Chem. Eng. Sci.*, 2006, **61**, 2192–2211.
- 9 W. Thomson (Lord Kelvin), *J. Math. Pures Appl.*, 1845, **10**, 364–367; W. Thomson (Lord Kelvin), *J. Math. Pures Appl.*, 1847, **12**, 256–264.
- 10 M. H. Davis, *Q. J. Mech. Appl. Math.*, 1964, **17**, 499–511.
- 11 T. Poppe and R. Schröpfer, *A&A*, 2005, **438**, 1–9.
- 12 Y. Liang, N. Hilal, P. Langston and V. Starov, *Adv. Colloid Interface Sci.*, 2007, **134–135**, 151–166.
- 13 W. S. Czarnecki and L. B. Schein, *Phys. Lett. A*, 2005, **339**, 145–151.
- 14 E. Bichoutskaia, A. L. Boatwright, A. Khachatourian and A. J. Stace, *J. Chem. Phys.*, 2010, **133**, 024105.
- 15 H. Zettergren, B. O. Forsberg and H. Cederquist, *Phys. Chem. Chem. Phys.*, 2012, **14**, 16360–16364.
- 16 T. Murovec and C. Brosseau, *Appl. Phys. Lett.*, 2013, **102**, 084105.
- 17 G. Raggi, A. J. Stace and E. Bichoutskaia, *Phys. Chem. Chem. Phys.*, 2013, **15**, 20115–20119.
- 18 A. Khachatourian, H. K. Chan, A. J. Stace and E. Bichoutskaia, *J. Chem. Phys.*, 2014, **140**, 074107.
- 19 H. Ohshima, *J. Colloid Interface Sci.*, 1998, **198**, 42–52.
- 20 R. Messina, *J. Chem. Phys.*, 2002, **117**, 11062–11074.
- 21 J. Q. Feng and D. A. Hays, *Powder Technol.*, 2003, **135–136**, 65–75.
- 22 T. P. Doerr and Y. K. Yu, *Phys. Rev. E: Stat., Nonlinear, Soft Matter Phys.*, 2006, **73**, 061902.
- 23 S. A. Khrapak, G. E. Morfill, V. E. Fortov, L. G. D'yachkov, A. G. Khrapak and O. F. Petrov, *Phys. Rev. Lett.*, 2007, **99**, 055003.

- 24 P. Linse, *J. Chem. Phys.*, 2008, **128**, 214505.
- 25 L. S. Matthews and T. W. Hyde, *IEEE Trans. Plasma Sci.*, 2004, **32**, 586–593.
- 26 J. Lekner, *Proc. R. Soc. A*, 2012, **468**, 2829–2848.
- 27 K. Kolikov, D. Ivanov, G. Krastev, Y. Epitropov and S. Bozhkov, *J. Electrostat.*, 2012, **70**, 91–96.
- 28 Z. Xu, *Phys. Rev. E: Stat., Nonlinear, Soft Matter Phys.*, 2013, **87**, 013307.
- 29 K. I. Popov, R. J. Nap, I. Szleifer and M. O. Cruz, *J. Polym. Sci., Part B: Polym. Phys.*, 2012, **50**, 852–862.
- 30 V. R. Munirov and A. V. Filippov, *J. Exp. Theor. Phys.*, 2013, **117**, 809–819.
- 31 M. Washizu and B. Techaumnat, *J. Electrostat.*, 2013, **71**, 854–861.
- 32 S. Atalay, M. Barisik, A. Beskok and S. Qian, *J. Phys. Chem. C*, 2014, **118**, 10927–10935.
- 33 A. J. Stace, A. L. Boatwright, A. Khachatourian and E. Bichoutskaia, *J. Colloid Interface Sci.*, 2011, **354**, 417–420.
- 34 W. R. Smythe, *Static and Dynamic Electricity*, McGraw-Hill, New York, 1950.
- 35 J. D. Jackson, *Classical Electrodynamics*, J. Wiley & Sons, London, 1962.
- 36 A. J. Stace and E. Bichoutskaia, *Phys. Chem. Chem. Phys.*, 2011, **13**, 18339–18346.
- 37 A. J. Stace and E. Bichoutskaia, *Soft Matter*, 2012, **8**, 6210–6213.
- 38 X. Chen, E. Bichoutskaia and A. J. Stace, *J. Phys. Chem. A*, 2013, **117**, 3877–3886.
- 39 H. K. Chan, E. B. Lindgren, A. J. Stace and E. Bichoutskaia, *Prog. Theor. Chem. Phys.*, 2015, **29**, 29–36.
- 40 P. M. Morse and H. Feshbach, *Methods of Mathematical Physics*, McGrawHill, 1953, vol. 2.
- 41 S. K. Sainis, V. Germain, C. O. Mejean and E. R. Dufrense, *Langmuir*, 2008, **24**, 1160.
- 42 S. K. Sainis, J. W. Merrill and E. R. Dufrense, *Langmuir*, 2008, **24**, 13334.